https://doi.org/10.5194/egusphere-2025-3062
Preprint. Discussion started: 14 July 2025

Revealing the Influence of Topography and Vegetation on Hydrological Processes Using a Stepwise Modelling Approach in Cold Alpine Basins of the Mongolian Plateau

Leilei Yong [1], Yahui Wang [1], Batsuren Dorjsuren [2], Zheng Duan [3], Hongkai Gao [1]*

[1] Key Laboratory of Geographic Information Science (Ministry of Education of China), School of Geographical Sciences, East China Normal University, Shanghai, China

[2] Department of Environment and Forest Engineering, National University of Mongolia, Ulaanbaatar 210646, Mongolia

[3] Department of Physical Geography and Ecosystem Science, Lund University, Sölvegatan 12, SE-223 62, Lund, Sweden

* Correspondence: Hongkai Gao, hkgao@geo.ecnu.edu.cn

Abstract: Topography and vegetation are critical factors influencing catchment hydrology; however, their individual contributions are often underestimated in hydrological models. This limitation is particularly evident in cold, mountainous regions such as the Mongolian Plateau, where observational data are sparse. To address this, we employed a stepwise, top-down modelling strategy based on the FLEX framework to systematically assess the influence of topography and vegetation on hydrological processes in the Bogd Uliastai and Zavkhan Guulin river basins. Beginning with a lumped model ($FLEX^L$), we successively integrated snow processes ($FLEX^L$-S), topographic distribution ($FLEX^D$), and finally, a landscape-based parameterization accounting for vegetation heterogeneity ($FLEX^T$). Both $FLEX^D$ and $FLEX^T$ outperformed the lumped models in simulating runoff and SWE. Interestingly, $FLEX^T$ showed similar performance to $FLEX^D$—likely due to limited vegetation heterogeneity—it offers more physically realistic parameterization by explicitly representing landscape units, suggesting its potential in more complex basins. Snowmelt contributions to streamflow were quantified as 23.5%±1.3% and 14.7%±1.6%

in the Bogd Uliastai and Zavkhan Guulin river basins, respectively, with peaks in spring and a clear increase with elevation. At high elevations, delayed snowmelt resulted in sustained runoff, while lower elevations responded more rapidly to rainfall. The explicit representation of vegetation heterogeneity further improved the model's capacity to capture landscape complexity and dominant hydrological mechanisms. This study underscores the pivotal roles of topography and vegetation in runoff generation and demonstrates the effectiveness of a stepwise modelling framework for improving hydrological understanding in cryospheric and data-scarce regions.

Keywords: Mongolian Plateau, FLEX model, stepwise modelling framework, snowmelt, topography, vegetation

1. Introduction

Understanding and accurately simulating hydrological processes are fundamental for elucidating basin hydrological patterns and supporting water resource management and ecological protection, especially under the context of global environmental change (Gomes et al., 2023; Oki and Kanae, 2006). Topography and vegetation play essential roles as drivers of hydrological processes, influencing key aspects such as precipitation, interception (Dwarakish and Ganasri, 2015), snowmelt (Hammond et al., 2019), evaporation (Jiao et al., 2017), and runoff generation (Qin et al., 2025). Topography governs water flow paths and moisture release processes (Gao et al., 2014), while vegetation affects water movement and infiltration by regulating precipitation interception and soil moisture dynamics (Zhu et al., 2022). The complex interaction between topography and vegetation not only define Hydrological Response Units (HRUs) but also shape the spatial heterogeneity and dominant hydrological mechanisms within a river basin (Savenije, 2010; Sivapalan, 2009). However, in cold-arid regions, data scarcity often leads to oversimplified hydrological models, limiting accurate simulations (Ragettli et al., 2014; Tarasova et al., 2016). Therefore, a more comprehensive evaluation of topography – vegetation interactions is essential for improving model fidelity and supporting effective water resource management and

https://doi.org/10.5194/egusphere-2025-3062
Preprint. Discussion started: 14 July 2025

ecological conservation.

Topography plays a fundamental role in shaping hydrological processes by influencing the spatial distribution of soil moisture, regulating precipitation patterns, modulating evaporation dynamics, and driving runoff generation, thereby governing the movement and storage of water across the landscape (Wicki et al., 2023). In mountainous basins, variations in topographic relief introduce substantial uncertainty into hydrological modeling (Seibert and McDonnell, 2002). Steeper slopes typically lead to more rapid runoff, while gentler slopes promote greater infiltration and moisture retention, thus affecting the spatial and temporal distribution of water resources (Ye et al., 2023). Moreover, topography critically influences snow distribution and snowmelt dynamics. Terrain features such as slope, aspect, and elevation induce spatial heterogeneity in snow accumulation and melting processes, resulting in diverse hydrological responses across the basin (Broxton et al., 2020).

Vegetation plays a crucial role in regulating hydrological processes, particularly through interception and root zone water storage. First, vegetation canopies intercept rainfall, reducing the amount of effective precipitation reaching the soil, while also mitigating surface erosion and slowing runoff (Cheng et al., 2020). Second, root zone storage capacity and plant transpiration regulate soil moisture, enhance evaporation and facilitating water redistribution (Luo et al., 2022; Volpe et al., 2013). These effects vary by vegetation type, as different structural forms (e.g., forests vs. grasslands) exhibit distinct hydrological behaviors (Chen et al., 2023). In cold mountainous regions, vegetation also affects snow processes by affecting snow distribution and retention. For example, forest canopies can shield snow accumulation, delay snowmelt, and reduce wind-driven redistribution, thereby significantly altering the spatiotemporal dynamics of meltwater runoff (Sun et al., 2022).

Although the regulatory role of topography and vegetation in basin hydrology are

https://doi.org/10.5194/egusphere-2025-3062
Preprint. Discussion started: 14 July 2025

widely acknowledged,, their synergistic interactions remain insufficiently understood, particularly in cold high-altitude mountainous regions characterized by complex terrain, harsh climatic conditions, and limited observational data (Stephens et al., 2021). Cryospheric regions serve as critical freshwater resources for downstream areas and are especially sensitive to changes in the hydrological cycle and climate (Immerzeel et al., 2010). In these regions, snowfall and snowmelt processes often dominate runoff generation, with topography and vegetation jointly modulating hydrological responses by influencing snow distribution, accumulation, and melt rates (Dharmadasa et al., 2023; Zhong et al., 2021). Therefore, quantifying the individual and combined effects of topography and vegetation, and effectively integrating them into hydrological models, is essential for advancing cold-region hydrology.

Existing hydrological models often struggle to adequately capture the complexities introduced by topography and vegetation. Early lumped models typically used basin-averaged precipitation and temperature to simulate runoff, thereby oversimplifying spatial heterogeneity within catchments (Beven, 2012). While computationally efficient, lumped models fail to accurately represent the spatial variability of terrain and land cover, especially in mountainous regions. The advent of distributed hydrological models has allowed more spatially explicit simulations by incorporating topographic and land cover data (Fenicia et al., 2016). However, the performance of these models is highly dependent on data quality, which remains a significant limitation in cold, high-mountain regions where traditional observations are sparse or unavailable.

Remote sensing has become an invaluable tool for providing high-resolution data on topography, vegetation, and snow in hydrological studies of cold regions. Digital elevation models (DEMs) offer critical topographic information such as slope, aspect, and elevation, while vegetation indices derived from remote sensing (e.g., NDVI and EVI) effectively characterize vegetation cover (Xiong et al., 2023). In addition, remote sensing techniques enable spatial monitoring of snow water equivalent and snowmelt

https://doi.org/10.5194/egusphere-2025-3062
Preprint. Discussion started: 14 July 2025

processes (Duethmann et al., 2014). Integrating remote sensing data with distributed hydrological models helps to overcome the limitations of traditional in-situ observations, offering a more comprehensive understanding of the roles that topography and vegetation play in shaping hydrological processes (Gao et al., 2014).

In the absence of direct measurements of individual hydrological processes, the top-down modelling approach offers a powerful means of exploring the internal dynamics of basin behavior (Fenicia et al., 2008b). Originally proposed by Klemes (Klemeš, 1983) and later reformulated by Sivapalan et al. (Sivapalan et al., 2003), the top-down approach is rooted in a deductive philosophy that infers the underlying 'causes' from the overall observed 'effect' of a system. In hydrological modeling, this method begins with a simple structure that is progressively refined to address limitations in reproducing observed catchment behavior (Fenicia et al., 2008a). In cold mountainous regions, the top-down approach holds significant potential for improving model realism by systematically incorporating key variables such as snow processes, topography, and vegetation.

This study focuses on the Bogd Uliastai and Zavkhan Guulin river basins on the Mongolian Plateau, aiming to investigate the roles of topography and vegetation in shaping hydrological processes in cold mountainous regions. Due to the scarcity of observational data, traditional hydrological models face significant challenges in these areas. To address this, we employ a top-down modelling approach, beginning with a lumped model to assess runoff dynamics and progressively advancing toward a distributed framework. This model explicitly incorporates key components—including snowmelt, topography, and vegetation—to better capture the hydrological responses of different landscape units. The study seeks to address three key research questions: (1) How can runoff be effectively simulated in data-scarce, cold mountainous regions using a top-down modelling approach? (2) How can the contribution of snowmelt to streamflow be quantified through a landscape-based hydrological model? (3) How do

https://doi.org/10.5194/egusphere-2025-3062
Preprint. Discussion started: 14 July 2025

topography and vegetation influence runoff generation processes?

2. Study site

2.1 Bogd Uliastai river basin

The Bogd Uliastai river basin (47°30′N-48°10′N, 96°45′E-97°45′E) is located in the northern part of the Zavkhan river headwaters, along the southern foothills of the central Khangaï Mountains in Mongolia (Fig.1). The basin spans an area of 1610 km^2 and is predominantly mountainous, with elevations ranging from 1753 m a.s.l to 3972 m a.s.l. The region receives an average annual precipitation of approximately 200 mm, with more than 80% of rainfall occurring between June and September. The average annual temperature is -1°C, while winter temperatures frequently fall below -30°C, reflecting a typical alpine climate. Runoff displays strong seasonal variability, with distinct peaks during the spring and summer and almost no flow in winter, resulting in extreme hydrological conditions (Dorjsuren et al., 2024). The vegetation exhibits clear altitudinal zonation: alpine meadows and tundra, dominated by mosses and lichens, prevail at higher elevations, whereas needlegrass steppe and low shrublands are common in mid- and low-elevation zones (Baasanmunkh et al., 2019).

https://doi.org/10.5194/egusphere-2025-3062
Preprint. Discussion started: 14 July 2025

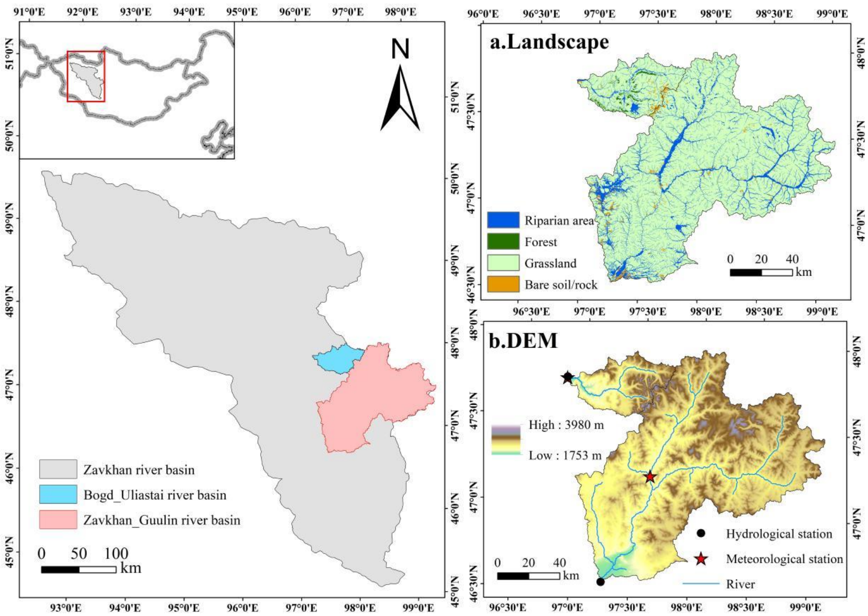

Fig.1 Location, landscape (a) and topography (b) of the Bogd Uliastai and Zavkhan Guulin river basins on the Mongolian Plateau.

2.2 Zavkhan Guulin river basin

The Zavkhan Guulin river basin (46°30′N-47°50′N, 96°45′E-97°00′E), located in the central and southern parts of Zavkhan Province, lies within the transitional zone of the southern Khangaï Mountains (Fig.1). The basin covers an area of approximately 12258 km^2 and is predominantly composed of low mountains and hills, with elevations ranging from 1785 m a.s.l. to 3980 m a.s.l. The basin's annual average precipitation is about 160 mm, with most precipitation concentrated in the summer, primaril in the form of heavy rain, which serves the main source of runoff. The annual average temperature is approximately -3°C, with summer temperatures exceeding 20°C and winter temperatures dropping as low as -50°C, characteristic of a temperate continental climate (Dorjsuren et al., 2023). Vegetation in the region is sparse, primarily dominated by drought-tolerant *Artemisia* species, with scattered distributions of grass and shrubs. At higher elevations, the landscape is characterized by alpine meadows, exposed rock surfaces, and cold desert environments. Soils are nutrient-poor, and the ecological

https://doi.org/10.5194/egusphere-2025-3062
Preprint. Discussion started: 14 July 2025

environment is fragile, facing severe challenges such as soil erosion (Baasanmunkh et al., 2019).

3. Data

3.1 Data set

Hydrometeorological data: Daily precipitation, runoff, and temperature data for the Bogd Uliastai river basin (2007–2015) and the Zavkhan Guulin river basin (2000–2020) were obtained from the Information and Research Institute of Meteorology, Hydrology, and Environment (IRIMHE) via its official website (http://irimhe.namem.gov.mn). For each basin, one meteorological station and one hydrological station served as the primary sources of observational data. The Arctic Snow Water Equivalent (SWE) Grid Dataset (2003–2016) was obtained from National Tibetan Plateau/Third Pole Environment Data Center (https://cstr.cn/18406.11.Snow.tpdc.271556). The SWE product has a daily temporal resolution and a spatial resolution of 10 km, covering latitudes from 45°N to 90°N and longitudes from 180°W to 180°E.

Topographic data: The Shuttle Radar Topography Mission Digital Elevation Model (SRTM-DEM), with a spatial resolution of 30 m, was acquired from the official website of the International Center for Tropical Agriculture (http://srtm.csi.cgiar.org).

Land cover data: The Sentinel-2 10-Meter Land Use/Land Cover was accessed via ESRI's official platform (https://livingatlas.arcgis.com/landcover/).

NDVI data: The normalized difference vegetation index (NDVI) data (2013–2020) were derived from the Landsat 8 Operational Land Imager (OLI) Level-2 surface reflectance products. NDVI was calculated as (NIR − Red)/(NIR + Red) using bands 5 (NIR) and 4 (Red). The dataset has a spatial resolution of 30 m and a temporal resolution of 16 days. Landsat data were obtained from the United States Geological Survey (USGS) EarthExplorer platform (https://earthexplorer.usgs.gov/).

3.2 Distribution of forcing data

https://doi.org/10.5194/egusphere-2025-3062
Preprint. Discussion started: 14 July 2025

Mountainous terrain is complex, and meteorological stations are typically located at lower elevations. Directly using point-based measurement in basin-scale simulations without accounting for elevation effects can introduce biases (Klemeš, 1989). In cold mountainous regions, higher elevations typically experience lower temperatures and greater precipitation, often in the form of snow (Lundquist et al., 2010; Stahl et al., 2006). In the study, the FLEX model divides catchment into elevation bands and adjusts temperature and precipitation for each band using a precipitation increase rate and temperature lapse rate. This distributed input approach effectively mitigates simulation bias by better capturing altitudinal variability in meteorological conditions. In this study, due to the remoteness of the region and the sparse distribution of meteorological stations, available ground observations were limited. Satellite and reanalysis products (e.g., ERA5) exhibit notable biases over complex terrain and fail to capture local climatic variability. We therefore relied on the best available in-situ data, which were subjected to rigorous quality control and spatial interpolation, and supplemented by topographic context and previous studies. While uncertainties remain, this approach provides the most reliable climate forcing achievable under current observational constraints. The model employed a precipitation increase rate of 4.2% per 100 m and a temperature lapse rate of 0.6°C per 100 m (Gao et al., 2014).

4. Modelling approach

4.1 Model description

To assess the impact of topography and vegetation on hydrological processes, this study designed and tested four conceptual models with increasing complexity: FLEX^L, FLEX^L-S, FLEX^D, and FLEX^T (Fig.2). The model structure and variables are shown in Fig. 2 and Table 1, and the water balance, isotope mass balance and constitutive equations are shown in Table 2.

https://doi.org/10.5194/egusphere-2025-3062
Preprint. Discussion started: 14 July 2025

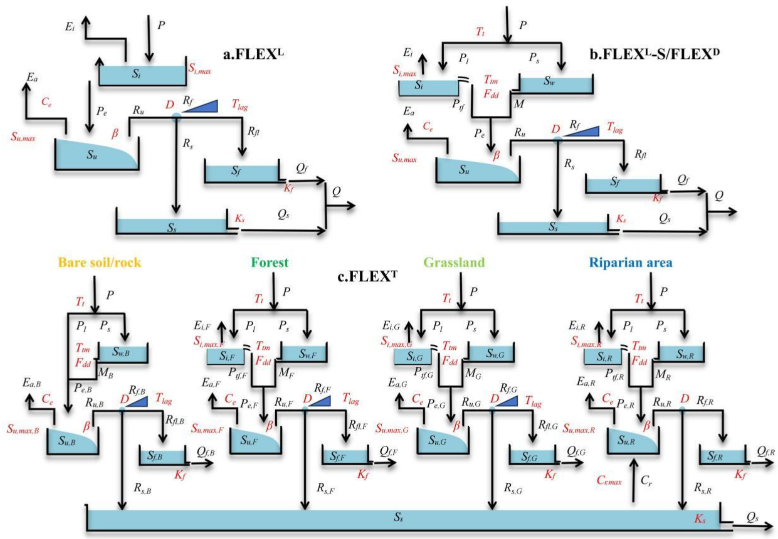

Fig.2 Stepwise modelling and the model structure of four models. (a) FLEX^{L} is a lumped model without snow module; (b) FLEX^{L}-S is a lumped model with snow module, and FLEX^{D} is a semi-distributed model with the same structure as FLEX^{L}-S. (c) FLEX^{T} is a landscape-driven semi-distributed model.

Table1. The variables of four models. In FLEX^{T} model, variables associated with various landscape categories are differentiated using specific suffixes, e.g., $E_{i,F}$, represent the interception from forest.

Variables	Meaning	Variables	Meaning
P (mm/d)	Precipitation	E_i (mm/d)	Interception
S_i (mm)	Interception reservoir	P_s (mm/d)	Snowfall
P_l (mm/d)	Rainfall	P_{tf} (mm/d)	Effective rainfall after interception
M (mm/d)	Snowmelt	P_e (mm/d)	Effective precipitation
S_u (mm)	Unsaturated reservoir	E_a (mm/d)	Actual evaporation
R_u (mm/d)	Generated runoff from the unsaturated reservoir	R_f (mm/d)	Generated fast runoff in the unsaturated zone
R_{fl} (mm/d)	Discharge into the fast response reservoir after the convolution	R_s (mm/d)	Generated slow runoff in the unsaturated zone
S_f (mm)	Fast response reservoir	S_s (mm)	Slow response reservoir
C_r (mm/d)	Capillary rise from groundwater into unsaturated reservoir on riparian area	Q_f (mm/d)	Subsurface storm flow
Q_s (mm/d)	Groundwater flow	Q (mm/d)	Total runoff

https://doi.org/10.5194/egusphere-2025-3062
Preprint. Discussion started: 14 July 2025

Table 2. The water balance and constitutive equations used in four models. Note: FLEX^L model lacks the snow module, resulting in different water balance and structural equations compared to other models. For FLEX^T model, in Eqs.(4), (6), and (7), the S_i and $S_{i,max}$ represent interception reservoir and their interception capacities in different landscapes, including forest ($S_{i,max,F}$), grassland ($S_{i,max,G}$) and riparian area ($S_{i,max,R}$) (There is no interception store in bare soil/rock area.). Similarly, in Eqs. (8), (10), (11), and (12), the S_u and $S_{u,max}$ represent root zone reservoirs and their storage capacities in different landscapes, including bare soil/rock ($S_{u,max,B}$), forest ($S_{u,max,F}$), grassland ($S_{u,max,G}$) and riparian area ($S_{u,max,R}$).

Reservoirs	Water balance equations	Constitutive equations
Interception reservoir (FLEX^L)	$\frac{dS_i}{dt} = P - E_i - P_e$ (1)	$E_i = min\left(E_p, min(P, S_{i,max})\right)$ (2) $P_e = max(P - E_i, 0)$ (3)
Snow reservoir (FLEX^L-S/FLEX^D/FLEX^T)	$\frac{dS_w}{dt} = P_s - M$ (4)	$P_s = \begin{cases} P; & T < T_t \\ 0; & T \geq T_t \end{cases}$ (5) $M = \begin{cases} F_{dd}(T - T_{tm}); & T > T_{tm} \\ 0; & T \leq T_{tm} \end{cases}$ (6)
Interception reservoir (FLEX^L-S/FLEX^D/FLEX^T)	$\frac{dS_i}{dt} = P_l - E_i - P_{tf}$ (7)	$P_l = \begin{cases} P; & T \geq T_t \\ 0; & T < T_t \end{cases}$ (8) $E_i = min\left(E_p, min(P_l, S_{i,max})\right)$ (9) $P_{tf} = max(P_l - E_i, 0)$ (10) $P_e = P_{tf} + M$ (11)

Unsaturated root zone reservoir (All)	$\frac{dS_u}{dt} = P_e - E_a - R_u$ (12)	$E_a = (E_p - E_i)min\left(\frac{S_u}{C_e S_{u,max}}, 1\right)$ (13) $R_u = \begin{cases} P_e - S_{u,max} + S_u + S_{u,max}\left(1 - \frac{P_e + AU}{(1+\beta)S_{u,max}}\right)^{(1+\beta)}; & (1+\beta)S_{u,max} > P_e + AU \\ P_e - S_{u,max} + S_u; & (1+\beta)S_{u,max} \le P_e + AU \end{cases}$ (14) $AU = (1+\beta)S_{u,max}\left(1 - \left(1 - \frac{S_u}{S_{u,max}}\right)^{\frac{1}{1+\beta}}\right)$ (15)
Splitter and lag function (All)		$R_f = R_u D$ (16) $R_S = R_u(1 - D)$ (17) $R_{fl} = \sum_{i=1}^{T_{lag}} c(i) \cdot R_f(t - i + 1)$ (18) $\mathrm{c(i)} = \mathrm{i}/\sum_{\mathrm{u=1}}^{\mathrm{T_{lag}}} \mathrm{u}$ (19)
Fast reservoir (All)	$\frac{dS_f}{dt} = R_f - Q_f$ (20)	$Q_f = S_f/K_f$ (21)
Slow reservoir (All)	$\frac{dS_s}{dt} = R_s - Q_s$ (22)	$Q_s = S_s/K_s$ (23)

https://doi.org/10.5194/egusphere-2025-3062
Preprint. Discussion started: 14 July 2025

4.1.1 $FLEX^L$

$FLEX^L$ is a lumped conceptual hydrological model composed of four reservoirs (Fig.2a): an interception reservoir (S_i), an unsaturated reservoir (S_u), a fast response reservoir (S_f), and a slow response reservoir (S_s). A lag function is used to represent the lag time from storm to peak flow (T_{lag}). $FLEX^L$ includes a total of 8 free calibration parameters (Table 3).

The interception reservoir was designed to simulate the process of precipitation interception by vegetation canopies or the ground surface (Eq.1). Interception evaporation (E_i) was calculated by potential evaporation (E_p) and S_i, considering the interception storage capacity ($S_{i,max}$) (Eq.2). When precipitation (P) exceeds $S_{i,max}$, the excess precipitation is routed as effective precipitation (P_e) into the unsaturated reservoir (Eq.3).

In the unsaturated reservoir, actual evaporation (E_a) was estimated based on E_p and root zone soil moisture ($S_u/S_{u,max}$) (Eq.13). The parameter C_e represents the threshold value controlling evaporation from the root zone soil moisture, and $S_{u,max}$ is root zone storage capacity. The water retention curve from the Xin'anjiang model was used to partition P_e into stored water in S_u and runoff generated from the unsaturated root zone (R_u) (Zhao, 1992) (Eqs.14 and 15).

In the response reservoir, a splitter D was applied to divide the R_u into two fluxes (R_f and R_s) (Eqs.16 and 17), and Eqs (18) and (19) were used to describe the lag time between storm and peak flow. $R_f(t-i+1)$ represents the fast runoff generated in the unsaturated zone at time $t-i+1$, T_{lag} represents the time lag between the storm and fast runoff generation. $c(i)$ is the weight of the flow in $i-1$ days before and $R_{fl}(t)$ is the discharge into the fast response reservoir after convolution. We used two linear reservoirs to represent the response process of subsurface storm flow (Q_f) and groundwater flow (Q_s) (Eqs.21 and 23).

https://doi.org/10.5194/egusphere-2025-3062
Preprint. Discussion started: 14 July 2025

4.1.2 FLEX^L-S

FLEX^L-S builds upon the FLEX^L model by incorporating a snow reservoir (S_w) to simulate the snow accumulation and melt processes (Fig.2b). When the daily air temperature exceeds the threshold temperature (T_t) and there is no snowpack (typically in summer), the interception process governs the initial partitioning of precipitation (Eq.7). In contrast, when the daily mean temperature is below T_t (normally occurs in winter), precipitation is stored as snow (Eq.5). When there is snowpack and the daily air temperature is above T_t (normally prevailing in early spring and early autumn), effective precipitation (P_e) is equal to the sum of effective rainfall after interception (P_{tf}) and snowmelt (M) (Eq.11). M was calculated by the snow degree day factor (F_{dd}) and the threshold temperature for melting (T_{tm}) (Eq.6) (Gao et al., 2017). In this study, T_{tm} was set to the same value as T_t. It is important to note that meltwater is conceptualized as directly infiltrating into the soil, thereby bypassing the interception reservoir.

4.1.3 FLEX^D

FLEX^D is a semi-distributed model with the same structure and parameters as FLEX^L-S (Fig.2b). Using DEM data, the Bogd Uliastai river basin was divided into 45 elevation bands with 50 m interval, while the Zavkhan Guulin river basin was divided into 44 elevation bands as shown in Fig.3. The FLEX^D model was operated with semi-distributed input data (see Sect.3.2), ensuring the integration of spatial variability into the model's processes.

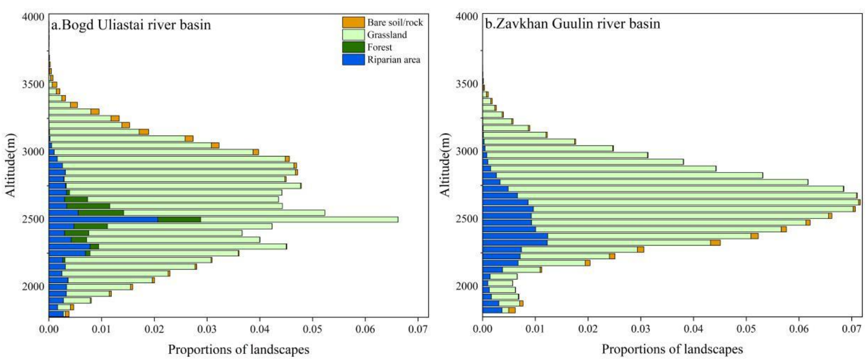

https://doi.org/10.5194/egusphere-2025-3062
Preprint. Discussion started: 14 July 2025

Fig.3 Area of different elevation and landscape in Bogd Uliastai and Zavkhan Guulin river basins.

4.1.4 FLEX^T

The FLEX^T model classified the Bogd Uliastai river basin into four landscape elements—bare soil/rock, forest, grassland, and riparian area—based on vegetation characteristics. In contrast, the Zavkhan Guulin river basin, which has no forest, was categorized into three landscape elements. By integrating both landscape types and elevation bands, the Bogd Uliastai river basin was further subdivided into 132 HRUs, while the Zavkhan Guulin river basin consisted of 117 HRUs (Fig.3).

The FLEX^T model's structure comprised four parallel components, representing the distinct hydrological functions associated with landscape elements (Savenije, 2010; Gao et al., 2014) (Fig.2c). To capture the diverse rainfall-runoff processes in different landscape types and simultaneously avoid over-parameterization, we kept the same model structure but gave different interception storage capacity ($S_{i,max}$) and root zone storage capacity ($S_{u,max}$) for all landscape elements (Table 3).

For forest, due to their dense vegetation cover and the greater amount of water required to fill the root zone to meet water deficits, larger prior ranges were assigned to $S_{i,maxF}$ and $S_{u,maxF}$. For bare soil/rock, due to no vegetation cover, we constrained a shallower $S_{u,maxB}$ and did not incorporate an interception module. For the riparian area, which is prone to saturation due to its location, we also constrained a shallower $S_{u,maxR}$, with the effect of capillary rise (C_r) taken into account. C_r is represented by a parameter ($C_{r,max}$) indicating a constant amount of capillary rise. Notably, the lag time from storm to peak flow was not considered in riparian area. For grasslands, $S_{u,maxG}$ is lower than that of forest but higher than bare soil/rock and riparian area.

https://doi.org/10.5194/egusphere-2025-3062
Preprint. Discussion started: 14 July 2025

Table 3. Uniform prior parameter distributions of four models. Note: $S_{i,max}$ and $S_{u,max}$ do not belong to the FLEX^{T} model.

Models				Parameter	Explanation	Prior range
				$S_{i,max}$ (mm)	Storage capacity of interception reservoir	(0.1, 2)
				$S_{u,max}$ (mm)	Root zone storage capacity	(5, 300)
				C_e (-)	Threshold controls actual evaporation and transpiration	(0, 1)
			FLEX^{L}	β (-)	Shape parameter of the tension water storage capacity curve	(0.1, 5)
				D (-)	Splitter between surface runoff and groundwater recharge	(0, 1)
	FLEX^{D}	FLEX^{L}-S		T_{lag} (-)	Time lag between storm and fast runoff generation	(0.8, 3)
				K_f (d)	Recession coefficient of fast response reservoir	(1, 10)
				K_s (d)	Recession coefficient of slow response reservoir	(10, 200)
				T_t (°C)	Threshold temperature to split snowfall and rainfall	(-2, 2)
				T_{tm} (°C)	Threshold temperature for melting	(-2, 2)
FLEX^{T}				F_{dd} (mm(°Cd)$^{-1}$)	Snow degree day factor	(1, 6)
				$S_{i,max}$ (mm)	Interception storage capacity of forest	(0.5, 2)
				$S_{i,max}$ (mm)	Interception storage capacity of grassland	(0.1, 1)
				$S_{i,max}$ (mm)	Interception storage capacity of riparian area	(0.1, 1)
				$S_{u,maxB}$ (mm)	Root zone storage capacity of bare soil/rock	(5, 120)
				$S_{u,maxF}$ (mm)	Root zone storage capacity of forest	(50, 300)
				$S_{u,maxG}$ (mm)	Root zone storage capacity of grassland	(10, 300)
				$S_{u,maxR}$ (mm)	Root zone storage capacity of riparian area	(5, 120)
				C_{Rmax} (mm/d)	Constant amount of capillary rise	(0.1, 2)

https://doi.org/10.5194/egusphere-2025-3062
Preprint. Discussion started: 14 July 2025

4.2 Snow contribution to streamflow

This study tracks the contribution of snowmelt to streamflow based on FLEX^T. The model assumes that snowmelt and rainfall mix rapidly and completely upon entering the model's conceptual reservoirs, thereby altering its internal composition ratios. The composition ratio of the water exiting the reservoir is identical to that within the reservoir. The contributions from snowmelt and rainfall represent portions of runoff generated at each time step, with some water remaining in the reservoir to participate in subsequent mixing, runoff generation, evaporation, and other hydrological processes (Liu et al., 2023). The method enables the tracking of the contribution of snowmelt to total runoff (C) at each time step by the following equation:

$$C = \frac{Q_M}{Q} = \frac{Q_{f,M} + Q_{s,M}}{Q} \tag{24}$$

$$Q_{f,M} = \frac{\left(\frac{M}{P_{tf}+M}\right) S_f}{K_f} \tag{25}$$

$$Q_{s,M} = \frac{\left(\frac{M}{P_{tf}+M}\right) S_s}{K_s} \tag{26}$$

where Q is total runoff in the river channel; Q_M is snowmelt runoff in the river channel; $Q_{f,M}$ is subsurface storm flow generated by snowmelt; $Q_{s,M}$ is groundwater flow generated by snowmelt.

4.3 Model calibration and uncertainty estimation

In the Bogd Uliastai river basin, the model was pre-warmed using data from 2007; the years 2008–2011 were used for calibration, and 2012–2015 for validation. In the Zavkhan Guulin river basin, 2000 was used as the warm-up year, with 2001–2010 selected for calibration and 2011–2020 for validation.

The MOSCEM-UA (Multi-objective Shuffled Complex Evolution Metropolis Algorithm) integrates multi-objective optimization and Bayesian uncertainty analysis, featuring global search capabilities that facilitate the generation of multiple Pareto

https://doi.org/10.5194/egusphere-2025-3062
Preprint. Discussion started: 14 July 2025

optimal solutions and provide an assessment of uncertainty (Vrugt et al., 2003). The MOSCEM_UA was run for the optimization of parameters, with 40000 iterations for four model structures. The model parameters and their prior ranges for calibration are listed in Table 3.

The Kling-Gupta Efficiency (KGE) and its logarithmic form (KGL) were used as objective functions to evaluate the simulation of daily discharge (Gupta et al., 2009). These two metrics were chosen because each emphasizes a different portion of the hydrograph: KGE is more sensitive to high-flow dynamics, while KGL better captures low-flow conditions. In this study, to accommodate minimization-based optimization algorithms, the runoff objective functions L_1 (Eq.27) and L_2 (Eq.28) were formulated as one minus their respective efficiency metrics. The two objective functions were assigned equal weights during model calibration to ensure a balanced representation of both high- and low-flow regimes.

$$L_1 = 1 - KGE = \sqrt{(1-\gamma)^2 + (1-\alpha)^2 + (1-\beta)^2} \quad (27)$$

$$L_2 = 1 - KGL = \sqrt{(1-\gamma_{log})^2 + (1-\alpha_{log})^2 + (1-\beta_{log})^2} \quad (28)$$

where, γ is the correlation coefficient between simulated and observed flows, and γ_{log} is the correlation coefficient between their logarithmic values; α is the ratio of the standard deviations of the simulated and observed flows, and α_{log} is the ratio of the standard deviations of their logarithmic transformations; β is the ratio of the mean values of the simulated and observed flows, and β_{log} is the ratio of the mean values of their logarithmic transformations.

5. Results and discussion

5.1 Model calibration and validation

Fig.4 shows the performance of the four models during the calibration period. The Pareto-optimal front shifts progressively toward the origin, indicating that model structural modifications enhance the model's ability to capture basin runoff dynamics. The FLEX^L-S model (KGE: 0.65 and 0.65, with the former representing the Bogd

https://doi.org/10.5194/egusphere-2025-3062
Preprint. Discussion started: 14 July 2025

Uliastai river basin and the latter representing the Zavkhan Guulin river basin, hereinafter referred to as the same; KGL: 0.68 and 0.66) (Table 4) outperforms the baseline FLEX^{L} model (KGE: 0.53 and 0.52; KGL: 0.62 and 0.48). This improvement highlights the importance of explicitly representing snow processes in cryospheric regions. Without accounting for snow accumulation and ablation, the model tends to overestimate minor peak flow events in winter, as shown in Fig.5, underscoring the critical role of snow dynamics in shaping hydrological responses.

The FLEX^{D} model (KGE: 0.77 and 0.68; KGL: 0.74 and 0.74) outperforms the FLEX^{L}-S, with the distributed precipitation and temperature inputs significantly improving the simulation of peak flow. Notably, FLEX^{D} does not require a more complex model structure or additional parameters compared to FLEX^{L}-S. However, it allows each hydrological response unit to maintain distinct storage states in the interception, snow, and unsaturated reservoirs on any given day. This capability effectively overcomes a key limitation of lumped models, which are unable to represent the spatial variability of hydrological responses across heterogeneous landscapes.

For hydrograph simulation, FLEX^{T} (KGE: 0.77 and 0.67; KGL: 0.74 and 0.75) performs comparably to FLEX^{D}. This similarity in performance—despite FLEX^{T}'s increased model complexity and more physically interpretable parameters—may be attributed to two main factors. First, both basins are dominated by grasslands, which cover more than 80% of the area, resulting in low vegetation heterogeneity (Fig.3). Second, vegetation characteristics—such as rooting depth and interception capacity—may already be implicitly represented by hydroclimatic and topographic variables (Antonelli et al., 2018; Roebroek et al., 2020), thereby diminishing the added value of explicitly incorporating vegetation information in this case.

As shown in Fig.6, the lumped model employs a spatially uniform NDVI value, which cannot reflect intra-basin vegetation variability. Nevertheless, a strong correspondence

https://doi.org/10.5194/egusphere-2025-3062
Preprint. Discussion started: 14 July 2025

is observed between elevation and NDVI, particularly in grassland-dominated regions. NDVI values across elevation bands closely match those of the corresponding grassland zones, suggesting that vegetation distribution is strongly aligned with topographic gradients. Although NDVI differs significantly between forested and bare land areas, these land cover types occupy only a small fraction of the basin and contribute negligibly to runoff generation. In this context, elevation can serve as a reliable proxy for vegetation structure, effectively embedding vegetation-related hydrological influence within the topographic representation. These findings support the notion that hydroclimatic and terrain-based variables may indirectly encode essential vegetation processes in distributed or semi-distributed models.

Together, these results suggest that the limited vegetation heterogeneity in the study basins may constrain the potential performance gains of FLEX^T over the simpler FLEX^D model. Nonetheless, the strength of FLEX^T lies in its explicit representation of distinct landscape units, enabling a more physically grounded simulation of hydrological processes and underlying mechanisms. Further research is warranted to evaluate the benefits of the landscape-based modeling approach in catchments with greater ecological and topographic complexity.

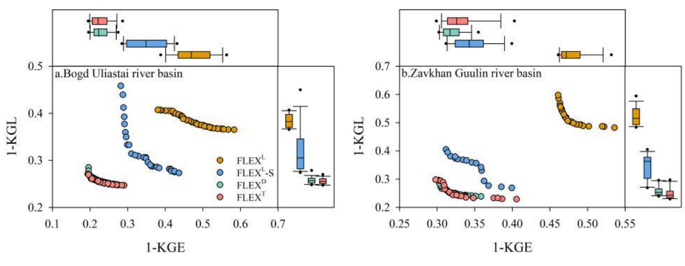

Fig.4 Performance of the FLEX^L, FLEX^L-S, FLEX^D, and FLEX^T models in calibration mode.

https://doi.org/10.5194/egusphere-2025-3062
Preprint. Discussion started: 14 July 2025

Table 4 Comparison of simulation performance among different hydrological models in the study catchments.

Basins	Evaluation indicators		Calibration				Validation			
			$FLEX^L$	$FLEX^L$-S	$FLEX^D$	$FLEX^T$	$FLEX^L$	$FLEX^L$-S	$FLEX^D$	$FLEX^T$
Bogd Uliastai river basin	KGE	Max	0.62	0.72	0.80	0.81	0.58	0.63	0.62	0.63
		Median	0.53	0.65	0.77	0.77	0.39	0.47	0.56	0.57
		Min	0.42	0.56	0.73	0.71	0.16	0.29	0.52	0.52
	KGL	Max	0.63	0.73	0.75	0.75	0.67	0.76	0.80	0.80
		Median	0.62	0.68	0.74	0.74	0.64	0.71	0.78	0.78
		Min	0.59	0.54	0.72	0.73	0.61	0.61	0.75	0.75
Zavkhan Guulin river basin	KGE	Max	0.54	0.69	0.70	0.70	0.41	0.59	0.62	0.64
		Median	0.52	0.65	0.68	0.67	0.31	0.47	0.56	0.56
		Min	0.46	0.60	0.64	0.59	0.13	0.28	0.41	0.40
	KGL	Max	0.52	0.73	0.76	0.77	0.60	0.73	0.74	0.76
		Median	0.48	0.66	0.74	0.75	0.56	0.66	0.72	0.73
		Min	0.40	0.60	0.70	0.70	0.47	0.61	0.70	0.69

Some interesting rain/snowmelt-runoff events also suggest that distributed models ($FLEX^D$ and $FLEX^T$) better capture basin hydrological processes. Two such events in the Bogd Uliastai river basin in April 2009 and September 2011 provide compelling evidence (Fig.5). In April 2009, despite minimal precipitation, temperatures exceeded the melting threshold, producing only a relatively insignificant peak flow. In September 2011, despite a higher daily precipitation of 12.7 mm, no runoff peak was observed within the basin. Lumped models failed to reproduce these dynamics accurately, instead simulating much larger peak flows. This limitation arises because lumped models do not account for elevation-dependent variations in temperature and precipitation type. When the average daily temperature exceeds the rain-snow separation (snowmelt) threshold, lumped models treat all precipitation as rain (snowmelt is assumed to occur uniformly across the entire basin). However, snowfall may still occur at higher elevations, where temperatures are below the threshold, resulting in limited snowmelt. Similarly, rainfall (and corresponding snowmelt) may occur in lower elevations even when the basin-average temperature falls below the threshold.

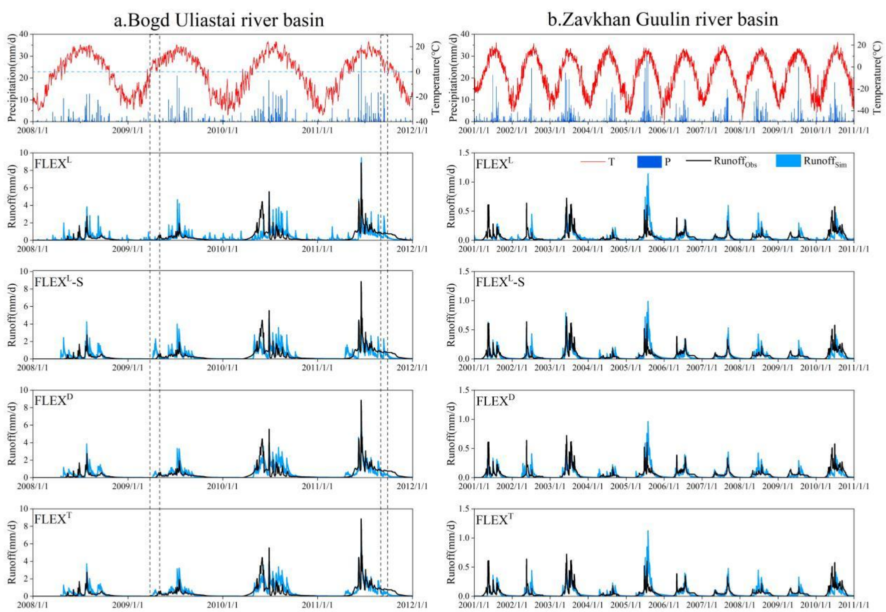

Fig.5 The daily observed and simulated hydrographs of the $FLEX^L$, $FLEX^L$-S, $FLEX^D$, and $FLEX^T$ models in the calibration period. The dashed boxes represent the rainfall/snowfall-runoff events in

https://doi.org/10.5194/egusphere-2025-3062
Preprint. Discussion started: 14 July 2025

April 2009 and September 2011 in the Bogd Uliastai river basin.

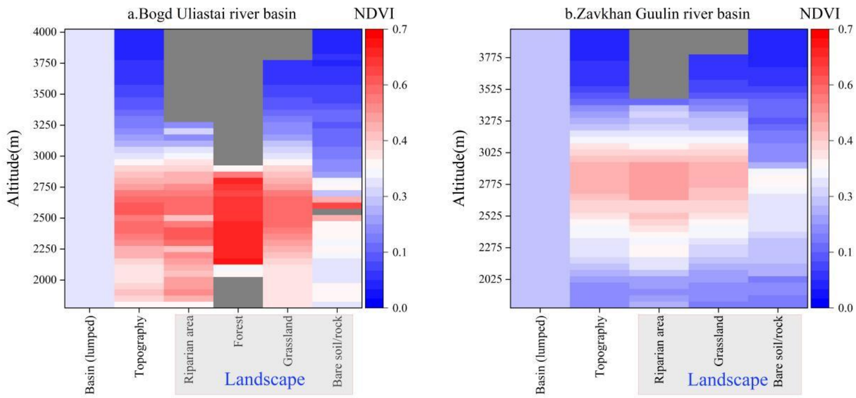

Fig.6 Multi-year average NDVI variation across landscapes and its relationship with elevation in two study basins.

The performance and results of the four models during the validation period are shown in Figs.7 and 8. The results confirm the stepwise improvement in model performance, as evidenced by the points corresponding to different model structures progressively shifting toward the origin. With the gradual optimization of model structure, the model's fitness has significantly improved. Unlike during calibration, the points in the validation period do not maintain the arc shape (Fig.4). This discrepancy is attributed to errors present in both the model and the data, the estimation of which remains a challenging task (Fenicia et al., 2008b).

In summary, a model's ability to reproduce basin-scale hydrological responses is governed not by the complexity of its structure or the sheer number of parameters, but by the relevance and accuracy of the hydrological processes it represents, and their influence on catchment-scale dynamics.

https://doi.org/10.5194/egusphere-2025-3062
Preprint. Discussion started: 14 July 2025

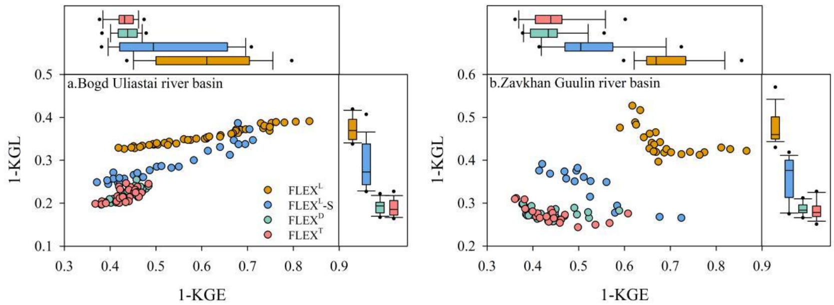

Fig.7 Performance of the FLEX^L, FLEX^L-S, FLEX^D, and FLEX^T models in validation mode.

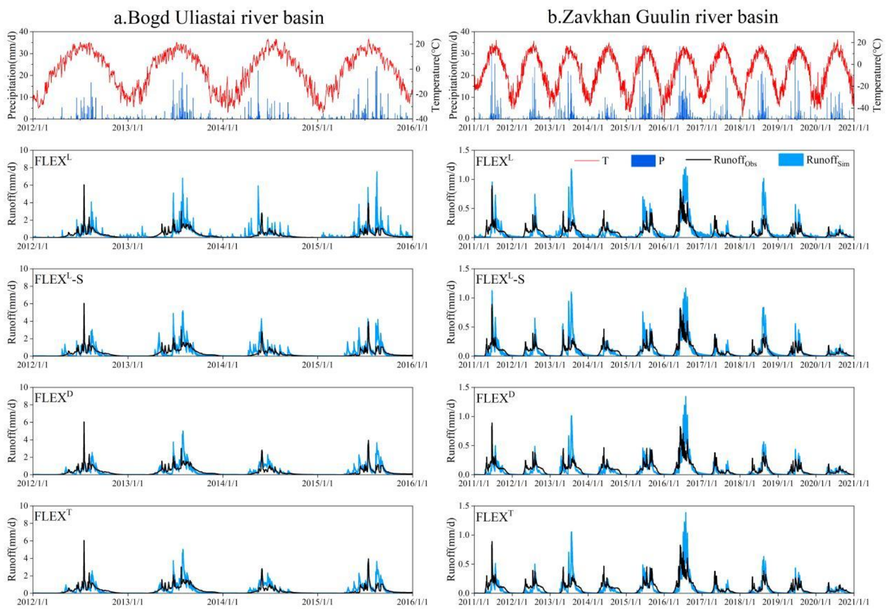

Fig.8 The daily observed and simulated hydrographs of the FLEX^L, FLEX^L-S, FLEX^D, and FLEX^T models in the validation period.

5.2 Model test by snowpack dynamics

Snow water equivalent is a crucial indicator of snowmelt dynamics and plays an essential role in hydrological modeling, serving as an additional metric for evaluating model performance and realism (Fig.9). In the Bogd Uliastai river basin, the FLEX^D and FLEX^T models achieved KGE values of 0.61 and 0.63, respectively, for SWE simulation, indicating their ability to capture seasonal patterns and interannual

https://doi.org/10.5194/egusphere-2025-3062
Preprint. Discussion started: 14 July 2025

variability, particularly peak values during winter and spring. The FLEX^T model, which incorporates vegetation effects, further improved SWE simulation accuracy and enhanced responsiveness to hydrological processes. In contrast, the FLEX^L-S model yielded a KGE of only 0.37, reflecting its limitations in capturing snowpack dynamics within the basin. Lumped models typically simplify the spatial heterogeneity of factors such as terrain and vegetation, limiting their ability to capture local-scale features and consequently reducing accuracy in complex environments (Bormann et al., 2009).

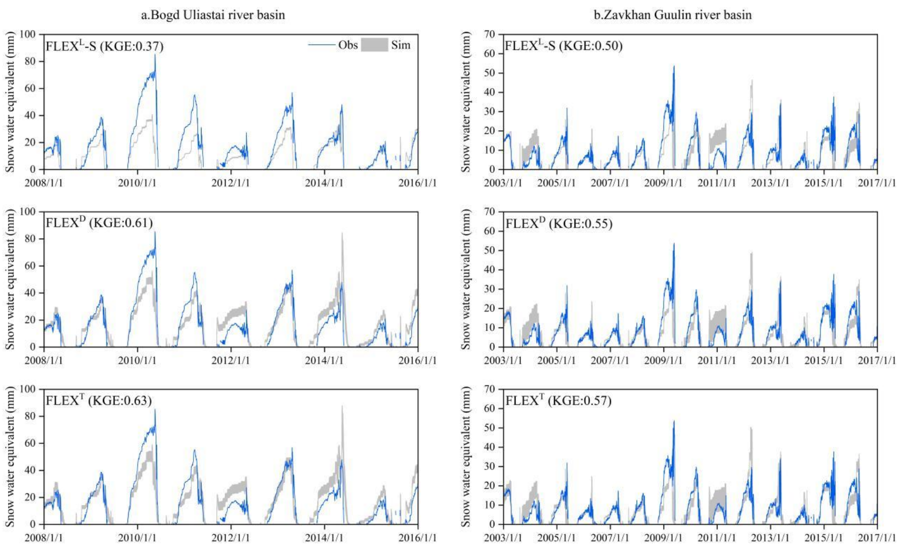

Fig.9 The observed and simulated daily snow water equivalent of the FLEX^L-S, FLEX^D, and FLEX^T models.

In the Zavkhan Guulin river basin, the FLEX^L-S model demonstrated relatively stable performance, achieving a KGE of 0.50. Although lumped models struggle to capture spatial heterogeneity, they effectively reflect seasonal precipitation and snowmelt trends. FLEX^D and FLEX^T achieved KGE values of 0.55 and 0.57, respectively, showed slight improvements. Model effectiveness remains strongly influenced by basin-specific climatic and landscape features—such as steep slopes, variable precipitation patterns, heterogeneous vegetation, and local climate fluctuations — all of which complicate accurate simulation of local-scale hydrological responses (Greco et al., 2023;

https://doi.org/10.5194/egusphere-2025-3062
Preprint. Discussion started: 14 July 2025

Nippgen et al., 2011). These challenges are further amplified in data-scarce, cold regions, where disentangling the interactions among these factors is particularly difficult (Chen et al., 2017). While current models provide valuable insights, further refinement and validation are necessary to better capture dynamic local processes and microclimatic effects.

5.3 Model parameters composition

A key feature of the stepwise modelling framework is the progressive refinement of parameterization towards greater physical realism. As shown in Fig.10, model parameters exhibit distinct sensitivity across different structural configurations. In models that do not account for vegetation effects, single parameter values are used to approximate basin-average hydrological behavior. By contrast, the FLEX^T model incorporates landscape-specific hydrological response characteristics, resulting in spatially differentiated parameter values that better reflect underlying process heterogeneity.

Forest, characterized by dense canopies, exhibit a higher value of $S_{i,maxF}$ (1.22 mm), effectively regulating water distribution during the initial stages of rainfall events (Wang et al., 2021). In comparison, $S_{i,maxG}$ (0.07 mm and 0.03 mm for the Bogd Uliastai and Zavkhan Guulin river basins, respectively) and $S_{i,maxR}$ (0.57 mm and 0.47 mm) are lower. The riparian area, however, shows greater interception capacity than grassland, likely due to denser or more abundant vegetation cover (Gao et al., 2014). Bare soil/rock surfaces lack interception capacity altogether, with rainfall either infiltrating directly into the ground or rapidly generating surface runoff along slopes.

For root zone storage capacity, $S_{u,maxF}$ is 150 mm, consistent with the findings of Wang-Erlandsson et al. (Wang-Erlandsson et al., 2016). Notable differences are observed in $S_{u,maxG}$ (54 mm and 283 mm) and $S_{u,maxR}$ (29 mm and 105 mm) under varying climatic conditions. $S_{u,maxB}$ (14 mm and 33 mm) exhibits the lowest values due to the absence of

https://doi.org/10.5194/egusphere-2025-3062
Preprint. Discussion started: 14 July 2025

vegetation cover and limited soil structure development (He et al., 2024).

The differences in interception and root zone storage capacity across landscapes between the two basins are primarily attributed to the more arid conditions in the Zavkhan Guulin river basin. This basin is characterized by sparse vegetation (reflected in lower $S_{i,max}$), higher evaporation losses (as suggested by greater $S_{u,max}$), and a low runoff coefficient of only 0.15.

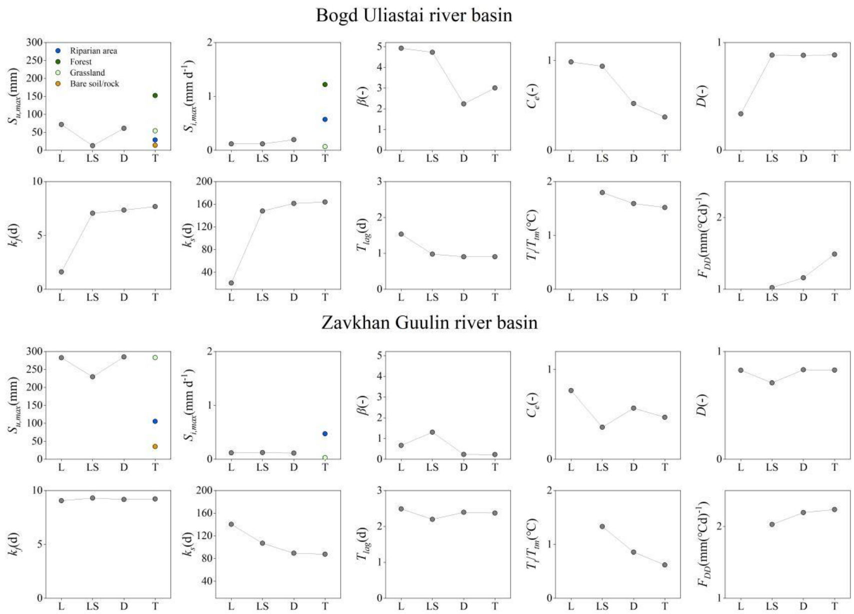

Fig.10 The changes of averaged behavioral parameters of the FLEX^{L}, FLEX^{L}-S, FLEX^{D}, and FLEX^{T} models.

Other parameters are also refined alongside improvements in the model structure. The parameter D, which partitions generated runoff between fast and slow response reservoirs, tends to be close to 1—indicating that most runoff is routed to the fast reservoir. This aligns with the observed runoff generation mechanisms in the study basins, which are primarily driven by intense rainfall events. Parameters related to energy processes, such as the T_{tm} and F_{dd}, exhibit a clear compensatory relationship: a higher T_{tm} is typically associated with a lower F_{dd}, and vice versa. This reflects model calibration trade-offs aimed at maintaining energy balance. Future work should

https://doi.org/10.5194/egusphere-2025-3062
Preprint. Discussion started: 14 July 2025

incorporate field observations to better quantify parameter heterogeneity across different landscape units. Such efforts would enhance both the physical interpretability and predictive robustness of the model.

5.4 Snow contribution to streamflow

Fig.11 shows the annual and seasonal contributions of snowmelt to streamflow in the Bogd Uliastai and Zavkhan Guulin river basins, as determined by the FLEX^T model. On an annual scale, snowmelt contributes 23.5%±1.3% and 14.7%±1.6% to streamflow in the Bogd Uliastai and Zavkhan Guulin river basins, respectively. Seasonally, snowmelt plays a dominant role in sustaining spring flows, while its contribution is considerably lower in other seasons. Although direct observational data (e.g., stable water isotopes) for quantifying snowmelt contributions are unavailable in this study, previous research provides indirect support. For example, Wu et al. (Wu et al., 2021) applied a similar snowmelt tracking method in the Altai Mountain and reported that snowmelt accounted for 29.3% of annual streamflow. This result exceeds those observed in our study, largely due to regional differences in snowfall. In the Kayiertesi river basin of the Altai Mountain, annual average precipitation for one hydrological year (September to August) was 409.8 mm from 2011 to 2015 (observed at the Kuwei snow station), with snowfall from November to March comprising about 31% of that annual precipitation (Zhang et al., 2017). In contrast, annual precipitation in the Bogd Uliastai and Zavkhan Guulin basins does not exceed 200 mm, and snowfall represents less than 15% of the total observed precipitation.

This study also compared model-based snowmelt tracking with traditional indirect methods, which estimate snowmelt contributions by calculating the ratio of snowfall or snowmelt to runoff over a given period (Barnett et al., 2005; Immerzeel et al., 2010). While computationally simple and data-efficient, these methods assume that all meltwater directly contributes to runoff, neglecting interactions with rainfall and losses due to infiltration, evaporation, and subsurface storage. Using the traditional indirect approach, we calculated the snowmelt-to-runoff ratios to be 38.8%±2.1% and

https://doi.org/10.5194/egusphere-2025-3062
Preprint. Discussion started: 14 July 2025

144.4%±20.1% in the two basins, respectively. These estimates are significantly higher than those obtained via model-based snowmelt tracking, with some values even exceeding 100%, indicating physical implausibility. This discrepancy highlights the limitations and scientific inadequacies of traditional methods. The overestimation likely arises from the failure to account for spatially disconnected snowmelt—specifically, snowmelt that infiltrates into the root zone and is subsequently lost through evaporation (Liu et al., 2023), particularly in the arid Zavkhan Guulin river basin. These findings underscore the importance of using physically based models to trace water source pathways, particularly in data-scarce and hydrologically complex regions.

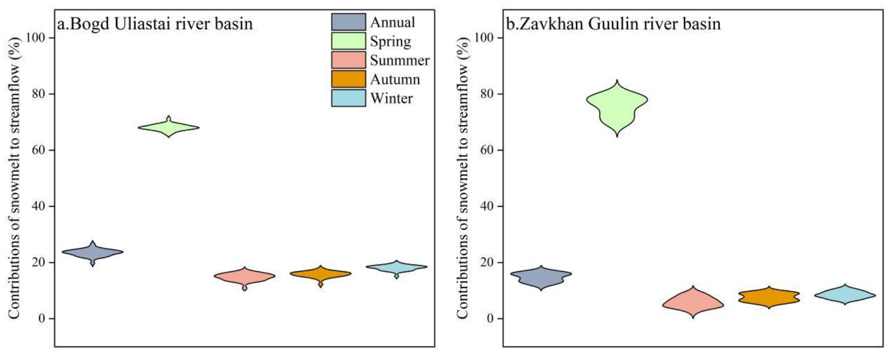

Fig.11 Contributions of snowmelt to streamflow (Q_M/Q) based on the FLEX^T model.

Fig.12 shows the snowmelt contribution to streamflow and the snowfall/precipitation ratio (P_s/P) across different elevations. The results indicate that the P_s/P increases significantly attributable to lower temperatures at higher altitudes that favor snowfall. Correspondingly, the contribution of snowmelt to streamflow also increases with elevation, directly linked to greater snow storage in high elevation areas, which providing a sustained water source for rivers (Sprenger et al., 2024). The finding underscores the decisive influence of snowmelt on streamflow in mountainous regions. With rising temperatures driven by climate change, low elevation areas may see more precipitation as rain, reducing snowpack, while accelerated snowmelt at higher elevations could increase the variability and instability of meltwater runoff

https://doi.org/10.5194/egusphere-2025-3062
Preprint. Discussion started: 14 July 2025

(Kraaijenbrink et al., 2021; Li et al., 2017).

Although the two basins share similar elevation and temperature regimes, their contrasting hydrological responses primarily reflect differences in climate and vegetation cover. The Bogd Uliastai river basin, dominated by mountainous grasslands, exhibits higher vegetation density (basin-average NDVI: 0.31; grassland NDVI: 0.34), whereas the Zavkhan Guulin river basin, situated in a semi-arid region, shows lower vegetation cover (basin-average NDVI: 0.26; grassland NDVI: 0.28) (Fig.6).

These vegetation differences influence snowmelt-runoff efficiency. In Bogd Uliastai river basin, the snowmelt contribution to streamflow closely matches the snowfall-to-precipitation ratio, indicating limited losses and effective runoff generation. By contrast, Zavkhan Guulin river basin experiences greater hydrological losses—primarily due to infiltration and evaporation—which cause snowmelt contributions to fall below the snowfall input, especially at higher elevations (Litaor et al., 2008).

Sparser vegetation and drier soils in Zavkhan Guulin river basin further enhance soil moisture retention, delaying runoff initiation and reducing the proportion of meltwater reaching the stream. This comparison highlights how subtle variations in vegetation structure, captured by NDVI, modulate hydrological partitioning and runoff efficiency across cold alpine landscapes (Zhong et al., 2021).

https://doi.org/10.5194/egusphere-2025-3062
Preprint. Discussion started: 14 July 2025

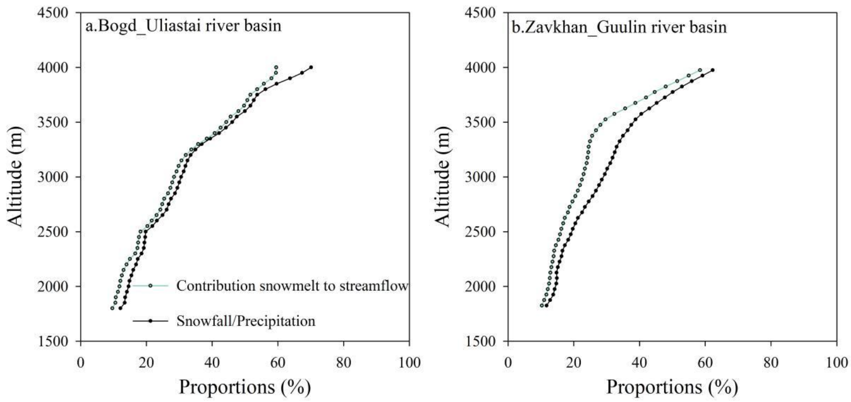

Fig.12 Contributions of snowmelt to streamflow (Q_M/Q) and snowfall/precipitation ratio (P_s/P) at different elevations based on FLEX^T model.

5.5 Runoff generation mechanisms at different elevation zones

Elevation is a key topographic factor influencing basin runoff processes and their seasonal variability, as it affects precipitation patterns, snow storage, and melt rates (Jenicek and Ledvinka, 2020). Fig.13 shows significant differences in runoff contributions across 5 equal area elevation bands. High elevation areas (above 2900 m or 2825 m) play a dominant role in runoff generation, primarily due to the orographic effect, which leads to increased precipitation and a higher proportion of snowmelt contributions (Ayala et al., 2023) (Fig.12). Runoff peaks in these high elevation areas are especially pronounced in spring and summer, highlighting the critical role of seasonal snowmelt. In contrast, low elevation areas rely primarily on rainfall-induced runoff. Due to limited precipitation and higher evaporative losses, their contributions to total runoff are comparatively smaller (Sprenger et al., 2022).

The lag effect in runoff is a notable characteristic of hydrological processes in mountainous basins, reflecting the differential responses of various elevation areas to hydrological drivers. In the Bogd Uliastai river basin, low elevation areas respond rapidly to precipitation events, contributing significantly to runoff during the early stages of peak flow. As the event progresses, contributions from higher elevation areas

https://doi.org/10.5194/egusphere-2025-3062
Preprint. Discussion started: 14 July 2025

gradually increase, highlighting the heterogeneous influence of elevation on runoff dynamics (Hajika et al., 2024). This lag is closely associated with delayed snowmelt process in high elevation areas. where lower temperatures cause precipitation to fall as snow. Snowmelt in these areas typically occurs weeks or even months later than in lower elevations, with the delay especially evident during the initial stages of the melt season (Gillan et al., 2010). A similar pattern is observed in the Zavkhan Guulin river basin, where runoff from high elevation continues to contribute significantly during the latter part of the hydrograph, thereby prolonging the recession phase (Fig.13).

The lag effect of runoff across different elevation areas has important implications for water resource management. In cold, high-mountain basins, the delayed hydrological response of upper elevation not only sustains downstream water supply during dry periods, but also significantly influences the timing and spatial extent of flood risk (Gu et al., 2023). During extreme precipitation events, rapid runoff generation in low-elevation areas may exacerbate short-term flood hazards, while delayed snowmelt from higher elevations can prolong flood durations. Therefore, both immediate and delayed hydrological responses should be holistically considered in catchment-scale management strategies (Li et al., 2019)

Although the lag effect is particularly evident during runoff peaks, current observational and modeling data remain insufficient to accurately quantify the specific response timings and processes across elevation gradients. Future research should integrate high-resolution numerical simulations with field-based observations to better disentangle the dynamic runoff contributions from different elevation areas, thereby enhancing the predictive skill and physical realism of hydrological models.

https://doi.org/10.5194/egusphere-2025-3062
Preprint. Discussion started: 14 July 2025

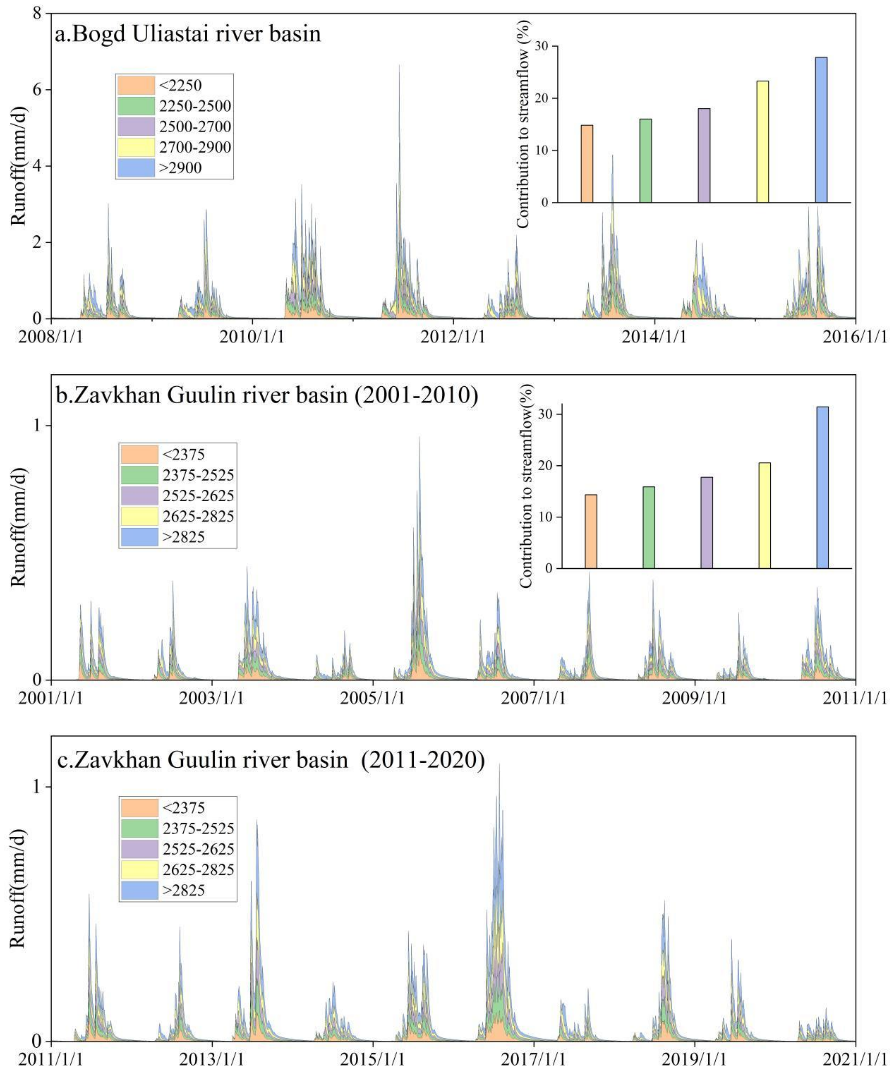

Fig.13 Runoff contribution from 5 equal area elevation bands (each representing 20% of the total catchment area) based on FLEX^{T} model.

5.6 Regulatory mechanisms of vegetation in runoff generation processes

Vegetation influences runoff generation not only through its direct physiological properties (e.g., interception, root zone storage, and transpiration), but also through its

https://doi.org/10.5194/egusphere-2025-3062
Preprint. Discussion started: 14 July 2025

spatial interactions with topography. To examine this regulatory role, we analyzed runoff responses across HRUs delineated by distinct vegetation types and elevation bands, thereby isolating process-driven variability from effects primarily driven by areal extent (Fig.14).

Despite grasslands occupying the largest portion of both basins (82.8% and 85.4%), their runoff generation capacity varies markedly with elevation and climatic context. In the more arid Zavkhan Guulin river basin, dry grassland soils exhibit high infiltration rates under unsaturated conditions, thereby reducing surface runoff. However, during peak melt or rainfall events, saturation thresholds are exceeded, triggering rapid surface runoff (Assouline et al., 2024).

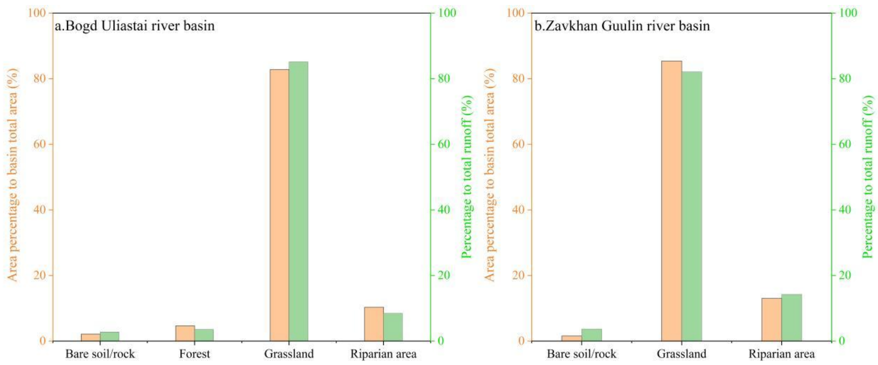

Fig.14 Runoff contribution from different landscapes based on FLEX^T model.

Riparian zones, although limited in area (10.3% and 13.0%), contribute disproportionately to runoff (8.5% and 14.2%) due to high soil moisture, shallow root zones, and strong hydrological connectivity. This is consistent with findings that riparian areas function as dynamic runoff buffers, responding rapidly to precipitation and snowmelt inputs (Leibowitz et al., 2023).

Forested areas, found only in the Bogd Uliastai basin, exhibit strong regulatory functions—intercepting precipitation, enhancing infiltration, and reducing quick flow generation (Liu et al., 2018; Stocker et al., 2023). These effects are particularly relevant under scenarios of climate-induced vegetation change.

https://doi.org/10.5194/egusphere-2025-3062
Preprint. Discussion started: 14 July 2025

The runoff generation capacity of bare soi/rock is high due to the lack of vegetation and low soil permeability. After rainfall or snowmelt, water infiltrates poorly and rapidly forms overland flow (Zeng et al., 2024). However, bare surfaces cover only a small portion of the catchment (2.2% and 1.6%), so their overall contribution to streamflow remains limited (2.8% and 3.7%). Despite their distinct hydrological behavior, bare areas play a secondary but notable role in runoff dynamics.

Importantly, our simulations reveal that interactions between vegetation and topography play a critical role in shaping runoff dynamics. At higher elevations, where vegetation is sparse and terrain is steep, snowmelt is rapidly converted into surface runoff due to limited soil storage capacity. In contrast, lower elevation areas dominated by grasslands and wetlands benefit from gentler slopes and deeper root zones, which enhance infiltration and delay runoff responses (Caviedes-Voullième et al., 2021).

These findings support the view that vegetation functions as a spatially variable regulator of runoff generation, contingent on topographic context and soil–plant–atmosphere interactions. This regulatory effect is particularly sensitive to future changes in vegetation cover and distribution under climate and land use change scenarios. For instance, overgrazing may reduce root zone storage capacity, thereby increasing runoff and erosion risks (Donovan and Monaghan, 2021). while shifts in vegetation type (e.g., shrub encroachment or forest decline) could alter hydrological partitioning along elevation gradients (Hsu et al., 2025; Zhou et al., 2023).

6 Conclusions

Hydrological modelling in high-latitude regions poses considerable challenges due to the complexity of cryospheric processes and limited observational data. To address these issues, this study proposes a stepwise modelling framework that incrementally refines model structures by incorporating key hydrological processes and landscape characteristics, thereby enhancing both the physical realism and predictive performance of the model.

Our results underscore the limitations of the lumped models ($FLEX^L$ and $FLEX^L$-S) in accurately representing runoff dynamics, particularly in regions with complex topography and heterogeneous vegetation cover. Although the distributed model $FLEX^D$ improved the simulation of runoff variability by incorporating spatially distributed inputs, it still lacks full physical interpretability of its parameters. In contrast, the landscape-based $FLEX^T$ model explicitly integrates snowpack, topography, and vegetation characteristics, thereby enhancing the physical realism of parameterization and offering a more mechanistic representation of hydrological processes. While $FLEX^T$ achieved performance comparable to $FLEX^D$ in simulating catchment runoff dynamics, this outcome may be attributed to the limited vegetation heterogeneity in the study basins. Nonetheless, validation using SWE confirmed $FLEX^T$'s capability to capture seasonal patterns, interannual variability, and key hydrological mechanisms in cryospheric environments. These findings underscore the potential advantages of $FLEX^T$, particularly in basins with greater ecological or topographic complexity.

Results from the $FLEX^T$ model indicate that snowmelt contributes 23.5%±1.3% and 14.7%±1.6% to streamflow in the Bogd Uliastai and Zavkhan Guulin river basins, respectively. Temporally, snowmelt contributions peak in spring and remain minimal during other seasons. Spatially, snowmelt contributions increase with elevation, underscoring the critical role of topography in shaping the spatiotemporal dynamics of runoff generation. In high elevation areas, the lagged snowmelt response leads to a sustained and gradual release of runoff, whereas low-altitude areas respond more rapidly to rainfall events. Moreover, hydrological modelling approaches based on vegetation landscape classifications better capture spatial heterogeneity and characterize the dominant hydrological mechanisms across different landscape units. These findings offer valuable insights into hydrological response mechanisms in cold alpine basins with limited observational data on the Mongolian Plateau. The stepwise modeling framework developed in this study not only improves the simulation of runoff dynamics in high-latitude regions but also enhances understanding of cryospheric hydrological responses to global climate change. Importantly, this framework holds both scientific and practical value, providing a foundation for more effective water resource management, ecological conservation, and climate adaptation in cryospheric and data-scarce regions.

Code availability

The code is available upon request to the contact author.

Data availability

All data presented in this manuscript are publicly available for download from: Hydrometeorological data (precipitation, runoff, temperature) from the Information and Research Institute of Meteorology, Hydrology, and Environment, available at http://irimhe.namem.gov.mn. Arctic Snow Water Equivalent Grid Dataset from the National Tibetan Plateau/Third Pole Environment Data Center, available at https://cstr.cn/18406.11.Snow.tpdc.271556. Shuttle Radar Topography Mission Digital Elevation Model (SRTM-DEM), available at http://srtm.csi.cgiar.org. Sentinel-2 10-meter Land Use/Land Cover data from the ESRI Living Atlas, available at https://livingatlas.arcgis.com/landcover/. NDVI data were obtained from the United States Geological Survey (USGS) EarthExplorer platform. available at https://earthexplorer.usgs.gov/.

Author contributions

LY and HG designed the study. BD provided the valuable fieldwork data. LY, YW, HG, and ZD conducted the analyses. LY wrote the paper. All authors discussed the results and the first draft and contributed to the final paper.

Competing interests

At least one of the (co-)authors is a member of the editorial board of Hydrology and Earth System Sciences.

Acknowledgments

This research is funded by National Key Research and Development Program of China (2024YFE0113200), the National Natural Science Foundation of China (grant no. 42471040). Zheng Duan would like to acknowledge the support from the Crafoord Foundation, Sweden (Grant No.20210552 and No.20240857). This work was performed as part of the IAHS HELPING Working Group on "Development & application of river basin simulators".

References

Antonelli, A. et al., 2018. Geological and climatic influences on mountain biodiversity. Nature Geoscience, 11(10): 718-725. DOI:10.1038/s41561-018-0236-z

Assouline, S., Sela, S., Dorman, M., Svoray, T., 2024. Runoff generation in a semiarid environment: The role of rainstorm intra-event temporal variability and antecedent soil moisture. Advances in Water Resources, 188: 104715. DOI:https://doi.org/10.1016/j.advwatres.2024.104715

Ayala, Á., Schauwecker, S., MacDonell, S., 2023. Spatial distribution and controls of snowmelt runoff in a sublimation-dominated environment in the semiarid Andes of Chile. Hydrol. Earth Syst. Sci., 27(18): 3463-3484. DOI:10.5194/hess-27-3463-2023

Baasanmunkh, S. et al., 2019. Contribution to the knowledge on the flora of northern Mongolia. Journal of Asia-Pacific Biodiversity, 12(4): 643-660. DOI:https://doi.org/10.1016/j.japb.2019.08.009

Barnett, T.P., Adam, J.C., Lettenmaier, D.P., 2005. Potential impacts of a warming climate on water availability in snow-dominated regions. Nature, 438(7066): 303-309. DOI:10.1038/nature04141

Beven, K.J., 2012. Rainfall-runoff modeling :the primer. Rainfall-runoff modelling: the primer, 15(1): 84-96.

Bormann, H., Breuer, L., Giertz, S., Huisman, J.A., Viney, N.R., 2009. Spatially explicit versus lumped models in catchment hydrology – experiences from two case studies. In: Baveye, P.C., Laba, M., Mysiak, J. (Eds.), Uncertainties in Environmental Modelling and Consequences for Policy Making. Springer Netherlands, Dordrecht, pp. 3-26.

Broxton, P.D., van Leeuwen, W.J.D., Biederman, J.A., 2020. Forest cover and topography regulate the thin, ephemeral snowpacks of the semiarid Southwest United States. Ecohydrology, 13(4): e2202. DOI:https://doi.org/10.1002/eco.2202

Caviedes-Voullième, D., Ahmadinia, E., Hinz, C., 2021. Interactions of Microtopography, Slope and Infiltration Cause Complex Rainfall-Runoff Behavior at the Hillslope Scale for Single Rainfall

Events. WATER RESOURCES RESEARCH, 57(7). DOI:10.1029/2020WR028127

Chen, J. et al., 2023. Differences in soil water storage, consumption, and use efficiency of typical vegetation types and their responses to precipitation in the Loess Plateau, China. Science of The Total Environment, 869: 161710. DOI:https://doi.org/10.1016/j.scitotenv.2023.161710

Chen, Y., Li, W., Fang, G., Li, Z., 2017. Review article: Hydrological modeling in glacierized catchments of central Asia – status and challenges. Hydrol. Earth Syst. Sci., 21(2): 669-684. DOI:10.5194/hess-21-669-2017

Cheng, X., Bai, Y., Zhu, J., Han, H., 2020. Effects of forest thinning on interception and surface runoff in Larix principis-rupprechtii plantation during the growing season. Journal of Arid Environments, 181: 104222. DOI:https://doi.org/10.1016/j.jaridenv.2020.104222

Dharmadasa, V., Kinnard, C., Baraër, M., 2023. Topographic and vegetation controls of the spatial distribution of snow depth in agro-forested environments by UAV lidar. The Cryosphere, 17(3): 1225-1246. DOI:10.5194/tc-17-1225-2023

Donovan, M., Monaghan, R., 2021. Impacts of grazing on ground cover, soil physical properties and soil loss via surface erosion: A novel geospatial modelling approach. Journal of Environmental Management, 287: 112206. DOI:https://doi.org/10.1016/j.jenvman.2021.112206

Dorjsuren, B. et al., 2024. Trend analysis of hydro-climatic variables in the Great Lakes Depression region of Mongolia. Journal of Water and Climate Change, 15(3): 940-957. DOI:10.2166/wcc.2024.379

Dorjsuren, B. et al., 2023. Hydro-Climatic and Vegetation Dynamics Spatial-Temporal Changes in the Great Lakes Depression Region of Mongolia, Water. DOI:10.3390/w15213748

Duethmann, D., Peters, J., Blume, T., Vorogushyn, S., Güntner, A., 2014. The value of satellite-derived snow cover images for calibrating a hydrological model in snow-dominated catchments in Central Asia. Water Resources Research, 50(3): 2002-2021. DOI:https://doi.org/10.1002/2013WR014382

Dwarakish, G.S., Ganasri, B.P., 2015. Impact of land use change on hydrological systems: A review of current modeling approaches. Cogent Geoscience, 1(1): 1115691. DOI:10.1080/23312041.2015.1115691

Fenicia, F., Kavetski, D., Savenije, H.H.G., Pfister, L., 2016. From spatially variable streamflow to distributed hydrological models: Analysis of key modeling decisions. Water Resources Research, 52(2): 954-989. DOI:https://doi.org/10.1002/2015WR017398

Fenicia, F., McDonnell, J.J., Savenije, H.H.G., 2008a. Learning from model improvement: On the contribution of complementary data to process understanding. Water Resources Research, 44(6). DOI:https://doi.org/10.1029/2007WR006386

Fenicia, F., Savenije, H.H.G., Matgen, P., Pfister, L., 2008b. Understanding catchment behavior through stepwise model concept improvement. Water Resources Research, 44(1). DOI:https://doi.org/10.1029/2006WR005563

Gao, H., Ding, Y., Zhao, Q., Hrachowitz, M., Savenije, H.H.G., 2017. The importance of aspect for modelling the hydrological response in a glacier catchment in Central Asia. Hydrological Processes, 31(16): 2842-2859. DOI:https://doi.org/10.1002/hyp.11224

Gao, H., Hrachowitz, M., Fenicia, F., Gharari, S., Savenije, H.H.G., 2014. Testing the realism of a topography-driven model (FLEX-Topo) in the nested catchments of the Upper Heihe, China. Hydrol. Earth Syst. Sci., 18(5): 1895-1915. DOI:10.5194/hess-18-1895-2014

Gillan, B.J., Harper, J.T., Moore, J.N., 2010. Timing of present and future snowmelt from high elevations

https://doi.org/10.5194/egusphere-2025-3062
Preprint. Discussion started: 14 July 2025

in northwest Montana. Water Resources Research, 46(1). DOI:https://doi.org/10.1029/2009WR007861

Gomes, M.N. et al., 2023. HydroPol2D — Distributed hydrodynamic and water quality model: Challenges and opportunities in poorly-gauged catchments. Journal of Hydrology, 625: 129982. DOI:https://doi.org/10.1016/j.jhydrol.2023.129982

Greco, R., Marino, P., Bogaard, T.A., 2023. Recent advancements of landslide hydrology. WILEY INTERDISCIPLINARY REVIEWS-WATER, 10(6). DOI:10.1002/wat2.1675

Gu, H. et al., 2023. Seasonal catchment memory of high mountain rivers in the Tibetan Plateau. Nature Communications, 14(1): 3173. DOI:10.1038/s41467-023-38966-9

Gupta, H.V., Kling, H., Yilmaz, K.K., Martinez, G.F., 2009. Decomposition of the mean squared error and NSE performance criteria: Implications for improving hydrological modelling. Journal of Hydrology, 377(1): 80-91. DOI:https://doi.org/10.1016/j.jhydrol.2009.08.003

Hajika, T., Yamakawa, Y., Uchida, T., 2024. Spatial distribution of rainfall–runoff characteristics and peak lag time in high-relief meso-scale mountain catchments where observations are scarce. Hydrological Processes, 38(6): e15177. DOI:https://doi.org/10.1002/hyp.15177

Hammond, J.C., Harpold, A.A., Weiss, S., Kampf, S.K., 2019. Partitioning snowmelt and rainfall in the critical zone: effects of climate type and soil properties. Hydrol. Earth Syst. Sci., 23(9): 3553-3570. DOI:10.5194/hess-23-3553-2019

He, S. et al., 2024. Impacts of re-vegetation on soil water dynamics in a semiarid region of Northwest China. Science of The Total Environment, 911: 168496. DOI:https://doi.org/10.1016/j.scitotenv.2023.168496

Hsu, J. et al., 2025. Impact of land use changes and global warming on extreme precipitation patterns in the Maritime Continent. npj Climate and Atmospheric Science, 8(1): 5. DOI:10.1038/s41612-024-00883-z

Immerzeel, W.W., van Beek, L.P.H., Bierkens, M.F.P., 2010. Climate Change Will Affect the Asian Water Towers. Science, 328(5984): 1382-1385. DOI:10.1126/science.1183188

Jenicek, M., Ledvinka, O., 2020. Importance of snowmelt contribution to seasonal runoff and summer low flows in Czechia. Hydrol. Earth Syst. Sci., 24(7): 3475-3491. DOI:10.5194/hess-24-3475-2020

Jiao, Y. et al., 2017. Impact of vegetation dynamics on hydrological processes in a semi-arid basin by using a land surface-hydrology coupled model. Journal of Hydrology, 551: 116-131. DOI:https://doi.org/10.1016/j.jhydrol.2017.05.060

Klemeš, V., 1983. Conceptualization and scale in hydrology. Journal of Hydrology, 65(1): 1-23. DOI:https://doi.org/10.1016/0022-1694(83)90208-1

Klemeš, V., 1989. The modelling of mountain hydrology : the ultimate challenge. IAHS-AISH publication, 190: 29-43.

Kraaijenbrink, P.D.A., Stigter, E.E., Yao, T., Immerzeel, W.W., 2021. Climate change decisive for Asia's snow meltwater supply. Nature Climate Change, 11(7): 591-597. DOI:10.1038/s41558-021-01074-x

Leibowitz, S.G. et al., 2023. National hydrologic connectivity classification links wetlands with stream water quality. Nature Water, 1(4): 370-380. DOI:10.1038/s44221-023-00057-w

Li, D., Lettenmaier, D.P., Margulis, S.A., Andreadis, K., 2019. The Role of Rain-on-Snow in Flooding Over the Conterminous United States. Water Resources Research, 55(11): 8492-8513. DOI:https://doi.org/10.1029/2019WR024950

https://doi.org/10.5194/egusphere-2025-3062
Preprint. Discussion started: 14 July 2025

Li, D., Wrzesien, M.L., Durand, M., Adam, J., Lettenmaier, D.P., 2017. How much runoff originates as snow in the western United States, and how will that change in the future? Geophysical Research Letters, 44(12): 6163-6172. DOI:https://doi.org/10.1002/2017GL073551

Litaor, M.I., Williams, M., Seastedt, T.R., 2008. Topographic controls on snow distribution, soil moisture, and species diversity of herbaceous alpine vegetation, Niwot Ridge, Colorado. Journal of Geophysical Research: Biogeosciences, 113(G2). DOI:https://doi.org/10.1029/2007JG000419

Liu, J., Zhang, Z., Zhang, M., 2018. Impacts of forest structure on precipitation interception and run-off generation in a semiarid region in northern China. Hydrological Processes, 32(15): 2362-2376. DOI:https://doi.org/10.1002/hyp.13156

Liu, Z., Cuo, L., Sun, N., 2023. Tracking snowmelt during hydrological surface processes using a distributed hydrological model in a mesoscale basin on the Tibetan Plateau. Journal of Hydrology, 616: 128796. DOI:https://doi.org/10.1016/j.jhydrol.2022.128796

Lundquist, J.D., Minder, J.R., Neiman, P.J., Sukovich, E., 2010. Relationships between Barrier Jet Heights, Orographic Precipitation Gradients, and Streamflow in the Northern Sierra Nevada. Journal of Hydrometeorology, 11(5): 1141-1156. DOI:https://doi.org/10.1175/2010JHM1264.1

Luo, Z. et al., 2022. Widespread root-zone water bypass for various climates and species: Implications for the ecohydrological separation understanding. Agricultural and Forest Meteorology, 324: 109107. DOI:https://doi.org/10.1016/j.agrformet.2022.109107

Nippgen, F., McGlynn, B.L., Marshall, L.A., Emanuel, R.E., 2011. Landscape structure and climate influences on hydrologic response. Water Resources Research, 47(12). DOI:https://doi.org/10.1029/2011WR011161

Oki, T., Kanae, S., 2006. Global Hydrological Cycles and World Water Resources. Science, 313(5790): 1068-1072. DOI:doi:10.1126/science.1128845

Qin, J., Yang, B., Ding, Y., Cui, J., Zhang, Y., 2025. Assessment of runoff generation capacity and total runoff contribution for different landscapes in alpine and permafrost watershed. CATENA, 249: 108643. DOI:https://doi.org/10.1016/j.catena.2024.108643

Ragettli, S., Cortés, G., McPhee, J., Pellicciotti, F., 2014. An evaluation of approaches for modelling hydrological processes in high-elevation, glacierized Andean watersheds. HYDROLOGICAL PROCESSES, 28(23): 5674-5695. DOI:10.1002/hyp.10055

Roebroek, C.T.J., Melsen, L.A., Hoek van Dijke, A.J., Fan, Y., Teuling, A.J., 2020. Global distribution of hydrologic controls on forest growth. Hydrol. Earth Syst. Sci., 24(9): 4625-4639. DOI:10.5194/hess-24-4625-2020

Savenije, H.H.G., 2010. HESS Opinions "Topography driven conceptual modelling (FLEX-Topo)". Hydrol. Earth Syst. Sci., 14(12): 2681-2692. DOI:10.5194/hess-14-2681-2010

Seibert, J., McDonnell, J.J., 2002. On the dialog between experimentalist and modeler in catchment hydrology: Use of soft data for multicriteria model calibration. Water Resources Research, 38(11): 23-1-23-14. DOI:https://doi.org/10.1029/2001WR000978

Sivapalan, M., 2009. The secret to ‘doing better hydrological science’: change the question! Hydrological Processes, 23(9): 1391-1396. DOI:https://doi.org/10.1002/hyp.7242

Sivapalan, M., Zhang, L., Vertessy, R., Blöschl, G., 2003. Downward approach to hydrological prediction. Hydrological Processes, 17(11): 2099-2099. DOI:https://doi.org/10.1002/hyp.1426

Sprenger, M. et al., 2022. Variability of Snow and Rainfall Partitioning Into Evapotranspiration and Summer Runoff Across Nine Mountainous Catchments. Geophysical Research Letters, 49(13): e2022GL099324. DOI:https://doi.org/10.1029/2022GL099324

https://doi.org/10.5194/egusphere-2025-3062
Preprint. Discussion started: 14 July 2025

Sprenger, M. et al., 2024. Stream water sourcing from high-elevation snowpack inferred from stable isotopes of water: a novel application of d-excess values. Hydrol. Earth Syst. Sci., 28(7): 1711-1723. DOI:10.5194/hess-28-1711-2024

Stahl, K., Moore, R.D., Floyer, J.A., Asplin, M.G., McKendry, I.G., 2006. Comparison of approaches for spatial interpolation of daily air temperature in a large region with complex topography and highly variable station density. Agricultural and Forest Meteorology, 139(3): 224-236. DOI:https://doi.org/10.1016/j.agrformet.2006.07.004

Stephens, C.M., Lall, U., Johnson, F.M., Marshall, L.A., 2021. Landscape changes and their hydrologic effects: Interactions and feedbacks across scales. Earth-Science Reviews, 212: 103466. DOI:https://doi.org/10.1016/j.earscirev.2020.103466

Stocker, B.D. et al., 2023. Global patterns of water storage in the rooting zones of vegetation. Nature Geoscience, 16(3): 250-256. DOI:10.1038/s41561-023-01125-2

Sun, N. et al., 2022. Forest Canopy Density Effects on Snowpack Across the Climate Gradients of the Western United States Mountain Ranges. WATER RESOURCES RESEARCH, 58(1). DOI:10.1029/2020WR029194

Tarasova, L., Knoche, M., Dietrich, J., Merz, R., 2016. Effects of input discretization, model complexity, and calibration strategy on model performance in a data-scarce glacierized catchment in Central Asia. Water Resources Research, 52(6): 4674-4699. DOI:https://doi.org/10.1002/2015WR018551

Volpe, V., Marani, M., Albertson, J.D., Katul, G., 2013. Root controls on water redistribution and carbon uptake in the soil–plant system under current and future climate. Advances in Water Resources, 60: 110-120. DOI:https://doi.org/10.1016/j.advwatres.2013.07.008

Vrugt, J.A., Gupta, H.V., Bouten, W., Sorooshian, S., 2003. A Shuffled Complex Evolution Metropolis algorithm for optimization and uncertainty assessment of hydrologic model parameters. Water Resources Research, 39(8). DOI:https://doi.org/10.1029/2002WR001642

Wang-Erlandsson, L. et al., 2016. Global root zone storage capacity from satellite-based evaporation. Hydrol. Earth Syst. Sci., 20(4): 1459-1481. DOI:10.5194/hess-20-1459-2016

Wang, G.X. et al., 2021. Critical advances in understanding ecohydrological processes of terrestrial vegetation: From leaf to watershed scale. CHINESE SCIENCE BULLETIN-CHINESE, 66(28-29): 3667-3683. DOI:10.1360/TB-2020-1339

Wicki, A., Lehmann, P., Hauck, C., Stähli, M., 2023. Impact of topography on in situ soil wetness measurements for regional landslide early warning – a case study from the Swiss Alpine Foreland. Nat. Hazards Earth Syst. Sci., 23(3): 1059-1077. DOI:10.5194/nhess-23-1059-2023

Wu, X. et al., 2021. Analysis of seasonal snowmelt contribution using a distributed energy balance model for a river basin in the Altai Mountains of northwestern China. Hydrological Processes, 35(3): e14046. DOI:https://doi.org/10.1002/hyp.14046

Xiong, C. et al., 2023. Improved global 250 m 8-day NDVI and EVI products from 2000–2021 using the LSTM model. Scientific Data, 10(1): 800. DOI:10.1038/s41597-023-02695-x

Ye, S. et al., 2023. From rainfall to runoff: The role of soil moisture in a mountainous catchment. Journal of Hydrology, 625: 130060. DOI:https://doi.org/10.1016/j.jhydrol.2023.130060

Zeng, X., Peng, X., Liu, T., Dai, Q., Chen, X., 2024. Runoff generation and erosion processes at the rock–soil interface of outcrops with a concave surface in a rocky desertification area. CATENA, 239: 107920. DOI:https://doi.org/10.1016/j.catena.2024.107920

Zhang, W., Kang, S.-c., Shen, Y.-p., He, J.-q., Chen, A.-a., 2017. Response of snow hydrological processes to a changing climate during 1961 to 2016 in the headwater of Irtysh River Basin, Chinese Altai Mountains. Journal of Mountain Science, 14(11): 2295-2310. DOI:10.1007/s11629-017-4556-z

Zhao, R., 1992. The Xinanjiang model applied in China. Journal of Hydrology, 135(1): 371-381. DOI:https://doi.org/10.1016/0022-1694(92)90096-E

Zhong, X.-Y. et al., 2021. Impacts of landscape and climatic factors on snow cover in the Altai Mountains, China. Advances in Climate Change Research, 12(1): 95-107. DOI:https://doi.org/10.1016/j.accre.2021.01.005

Zhou, S., Yu, B., Lintner, B.R., Findell, K.L., Zhang, Y., 2023. Projected increase in global runoff dominated by land surface changes. Nature Climate Change, 13(5): 442-449. DOI:10.1038/s41558-023-01659-8

Zhu, G. et al., 2022. Evaporation, infiltration and storage of soil water in different vegetation zones in the Qilian Mountains: a stable isotope perspective. Hydrol. Earth Syst. Sci., 26(14): 3771-3784. DOI:10.5194/hess-26-3771-2022